

AD-A141 869

ZINC SELENIDE PHOTODELCTRODES EFFICIENT RADIATIVE
RECOMBINATION IN A STAB. (U) WISCONSIN UNIV-MADISON
DEPT OF CHEMISTRY P M SMILEY ET AL. 25 MAY 84

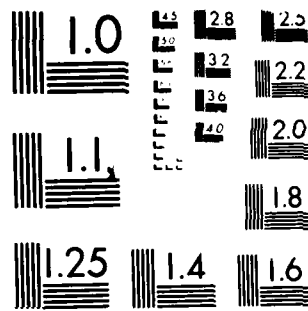
UNCLASSIFIED UWIS/DC/TR-84/1 N00014-78-C-0633

1/1

F/G 10/2

NL

END
15TH
FILMED
7-84
DTIC



MICROCOPY RESOLUTION TEST CHART
NATIONAL BUREAU OF STANDARDS 1964

AD-A141 869

(12)

OFFICE OF NAVAL RESEARCH
Contract No. N00014-78-C-0633
Task No. NR 051-690
TECHNICAL REPORT No. UWIS/DC/TR-84/1

Zinc Selenide Photoelectrodes. Efficient Radiative Recombination
in a Stable Photoelectrochemical Cell

by

Patricia M. Smiley, Richard N. Biagioni, and Arthur B. Ellis

Prepared for Publication

in

Journal of the Electrochemical Society

Department of Chemistry
University of Wisconsin
Madison, Wisconsin 53706

May 25, 1984

Production in whole or in part is permitted
for any purpose of the United States Government

Approved for Public Release: Distribution
Unlimited

DTIC
ELECTE
S JUN 07 1984 D
E

84 06 06 006

DTIC FILE COPY

Unclassified

SECURITY CLASSIFICATION OF THIS PAGE (When Data Entered)

REPORT DOCUMENTATION PAGE		READ INSTRUCTIONS BEFORE COMPLETING FORM
1. REPORT NUMBER UWIS/DC/TR-84/1	2. GOVT ACCESSION NO. AD-A141869	3. RECIPIENT'S CATALOG NUMBER
4. TITLE (and Subtitle) Zinc Selenide Photoelectrodes. Efficient Radiative Recombination in a Stable Photoelectrochemical Cell		5. TYPE OF REPORT & PERIOD COVERED
7. AUTHOR(s) Patricia M. Smiley, Richard N. Biagioni, and Arthur B. Ellis		6. PERFORMING ORG. REPORT NUMBER
8. CONTRACT OR GRANT NUMBER(s) N00014-78-C-0633		9. PERFORMING ORGANIZATION NAME AND ADDRESS Department of Chemistry, University of Wisconsin, Madison, Wisconsin 53706
11. CONTROLLING OFFICE NAME AND ADDRESS Office of Naval Research/Chemistry Program Arlington, Virginia 22217		10. PROGRAM ELEMENT, PROJECT, TASK AREA & WORK UNIT NUMBERS NR 051-690
14. MONITORING AGENCY NAME & ADDRESS (if different from Controlling Office)		12. REPORT DATE May 25, 1984
		13. NUMBER OF PAGES 22
		15. SECURITY CLASS. (of this report)
		15a. DECLASSIFICATION/DOWNGRADING SCHEDULE
16. DISTRIBUTION STATEMENT (of this Report) Approved for Public Release: Distribution Unlimited		
17. DISTRIBUTION STATEMENT (of the abstract entered in Block 20, if different from Report)		
18. SUPPLEMENTARY NOTES Prepared for publication in the Journal of the Electrochemical Society		
19. KEY WORDS (Continue on reverse side if necessary and identify by block number) photoluminescence, electroluminescence, zinc selenide electrodes, photoelectrochemistry		
20. ABSTRACT (Continue on reverse side if necessary and identify by block number) Photoluminescence (PL) and electroluminescence (EL) from single-crystal, n-type, Al-doped ZnSe (ZnSe:Al) electrodes have been studied. These samples exhibit both edge emission ($\lambda_{\text{max}} \sim 460$ nm) and subband gap emission when excited at several ultraband-gap wavelengths. The latter PL band is particularly intense, with a measured radiative quantum yield of $\sim 10^{-1}$ to 10^{-2} . The transition seems at least partially self-activated (SA) in origin, based on previously reported PL data. Excited-state communication involving the		

Unclassified

SECURITY CLASSIFICATION OF THIS PAGE (When Data Entered)

two emissive states is inferred from time-resolved PL measurements. Stable photoelectrochemical cells (PEC's) can be constructed from n-ZnSe:Al electrodes and aqueous diselenide or ditelluride electrolytes. Applied potential quenches both of the photoanodes' PL bands roughly in parallel. The extent of PL quenching is consistent with a dead-layer model previously used to describe quenching in Au-ZnSe Schottky diodes. When used as a dark cathode in aqueous, alkaline peroxydisulfate electrolyte, EL from ZnSe:Al electrodes is observed. PL and EL spectral distributions are similar and indicate that the same emissive excited states are populated in the two experiments. Measured EL efficiencies, $\sim 10^{-4}$ to 10^{-6} at -2.2 and -1.8 V vs. SCE, respectively, are much smaller than PL efficiencies. Possible sources of the discrepancies are discussed.

Accession For	
NTIS GRA&I	<input checked="" type="checkbox"/>
DTIC TAB	<input type="checkbox"/>
Unannounced	<input type="checkbox"/>
Justification	
By _____	
Distribution/ _____	
Availability Codes	
Dist	Avail and/or Special
A-1	



Unclassified

SECURITY CLASSIFICATION OF THIS PAGE (When Data Entered)

Keen interest in photoelectrochemical cells (PEC's) has focused attention on the excited-state properties of the semiconductor electrodes which serve as the key element of these devices (1). We and others have studied photoluminescence (PL) and electroluminescence (EL) from a variety of II-VI and III-V semiconductor electrodes in an effort to determine the effect of PEC parameters on the solids' excited-state deactivation routes (2). In general, measured radiative quantum yields, ϕ_r , of these materials have been small, $\sim 10^{-3}$ - 10^{-5} . We describe in this paper an electrode, n-ZnSe:Al, whose emission competes very favorably ($\phi_r \sim 10^{-1}$ - 10^{-2}) with other deactivation paths in stable, efficient PEC's. As observed with other semiconductor electrodes (3), the PL of n-ZnSe:Al electrodes can be perturbed and EL initiated by interfacial charge-transfer processes. We show that PL quenching by applied potential is compatible with a dead-layer model used to describe such quenching in other PEC's (4,5) and in Au-ZnSe Schottky diodes (6).

Experimental

Materials. Single-crystal (111) plates of n-type ZnSe:Al (~ 2 ppm Al based on arc emission spectroscopy) were generously provided by North American Philips Corp., Briarcliff Manor, N.Y.; the samples ($\sim 5 \times 5 \times 0.25$ mm) had been cut from boules which were obtained from Eagle-Picher Industries, Miami, OK and had been subsequently heat-treated in molten Zn at 950°C for 24 h to lower their resistivity to ~ 1 - 10 ohm-cm. Twinned areas may be present below the surface in some of the samples employed. Sample carrier concentrations of $\sim 10^{17}$ - 10^{18} cm^{-3} were estimated from both dc Hall measurements (7) and Mott-Schottky data. In the former measurement, a Varian Associates Model V-2301-A dc electromagnet producing a field of ~ 0.5 kG was employed. Capacitance measurements of the ZnSe:Al electrodes were made at 1.0 and 0.8 kHz in 1M OH^- and diselenide electrolytes, respectively, using an Ithaco Dynatrac 391 lock-in voltmeter, EG&G PAR Models 173 potentiostat and 175 programmer, and a Wavetek Model 182A 4MHz function generator. Electrodes were prepared by etching the solids for 20 s with $1:40$ Br_2/MeOH (v/v), making ohmic contact to the Se-rich crystal face by soldering with In, and then mounting the solid as an electrode as described previously (8).

Resistivity in some samples was deliberately enhanced by heat-treatment with Se (Alfa; m3N purity). For these experiments, an \sim 10-mg sample of ZnSe:Al was placed in a quartz tube with \sim 0.2 mg of Se. The quartz ampule was evacuated (\sim 0.1 Torr), sealed to a volume of \sim 3 cm³, and heated at 700°C in a Lindberg furnace for \sim 30 s. After its removal from the ampule, the solid was etched until bright PL was observed, then mounted as an electrode. Sulfide, diselenide and ditelluride electrolytes were prepared as described previously (9,10), except that after the solid Na₂Se was washed with NaOH, it was dissolved in conc. KOH to yield solutions whose compositions were \sim 10M KOH/0.25M Se²⁻. During PEC experiments, the electrolytes were vigorously stirred and blanketed with N₂. Preparation of peroxydisulfate electrolyte has been described (11). MgO powder was obtained from Baker Chemical Co.

PL Properties. Front-surface PL spectra at ambient temperature and at 77 K were obtained with the Aminco-Bowman spectrophotofluorometer described previously (3). The high-pressure Xe lamp of the instrument was used in conjunction with an interference filter (Edmund Scientific) for 405-nm excitation; a Corning 3-72 filter was used to prevent this light from reaching the detection optics. All PL and EL spectra were corrected for detector sensitivity from 350 nm to 800 nm using a procedure previously described (3). The correction factors were incorporated into a computer program for use with an APPLE II Plus Computer. Spectra were digitized, corrected by the program, and plotted on an EPSON printer.

Measurements of ϕ_r were made by placing the ZnSe:Al samples and MgO powder (reference) in turn in a quartz cuvette positioned in the Aminco-Bowman spectrometer's sample compartment as previously described (3,12). The sample was irradiated "head-on" with the spectrometer's high-pressure Xe lamp; interference filters (FWHM is \sim 10 nm except for 366 nm where it is \sim 30 nm) were used to isolate the desired excitation wavelengths. Both the reflected and emitted intensities were corrected for relative detector response.

The dependence of ϕ_r on incident intensity was probed using the near uv lines of a Coherent Radiation CR-12 Ar⁺ laser (351-and 364-nm doublet). Samples were mounted with epoxy on a glass rod and positioned at $\sim 45^\circ$ to both the laser beam and the emission detection optics. PL spectra were run as a function of incident intensity which was varied with Melles Griot neutral density filters; the EG&G radiometer was used to measure incident intensity in conjunction with a glass slide which served as a beam splitter.

Time-resolved PL data were obtained in air with a pulsed N₂ laser (337 nm) and N₂-pumped dye laser (460 nm) using instrumentation and techniques previously reported (13). Peak intensities of ~ 3 and 30 kW/cm² were used in these experiments with essentially no difference in the resulting decay curves.

PEC Experiments. A flat-faced quartz cell equipped with a side arm was employed for most PEC measurements. Long-term stability experiments in diselenide and ditelluride electrolytes were conducted as described previously with an n-ZnSe:Al working electrode and a Pt foil counterelectrode (8). A polyethylene bag was attached to the top of the cell and purged with N₂ during the experiments.

Photoaction spectra were obtained as previously described (14) using transparent selenide electrolyte. The output of a 150-W Xe lamp (Oriel) was monochromatized for excitation; lamp intensity was measured with the EG&G radiometer whose response from 350-800 nm was corrected with the manufacturer's calibration factors. Photocurrents were measured at -1.0 V vs. SCE.

A standard three-electrode potentiostatic setup was used for obtaining iV data. Excitation at 366, 405, and 436 nm (200-W, high-pressure Osram Hg lamp with interference filters) was used; lenses and masks were used to fill the exposed electrode area with light. Electrochemical measurements were made with an EG&G PAR Model 174 potentiostat; i-V curves were recorded on a Houston Model 2000 x-y recorder. Steady-state PL intensity in operating PEC's was influenced by production of colored Se₂²⁻ and Te₂²⁻ species. A pulse technique

was employed to minimize this problem during the generation of iLV curves. The technique consisted of pulsing the electrode between open circuit and increasingly positive potentials. Typically, the electrode sat at open circuit for 500 ms, then was pulsed for 57 ms to a potential which increased by 5 mV with each cycle. The i-V curves obtained in this manner were identical to steady-state i-V curves. PL was detected with the EG&G radiometer covered by a 600-nm interference filter. Output signals were displayed on a Tektronix Model RM503 oscilloscope equipped with a camera; sweep rates which resulted in potential steps of \sim 10 mV/s permitted an entire PL intensity-V curve to be photographed with one exposure of \sim 2 min. Incident light intensity was measured by inserting a mirror (\sim 80% reflectivity) and reflecting the light into the EG&G radiometer. The weakness of the edge PL required use of the near-uv lines of the Ar⁺ laser and the Aminco-Bowman spectrometer for generation of iLV curves in which both PL bands could be monitored.

EL Properties. EL spectra were obtained in 5M NaOH/0.1 M K₂S₂O₈ electrolyte by pulsing the electrode between 0.00 V (8 s) and a potential cathodic of \sim 1.7 V vs SCE (1 s), while slowing scanning the monochromator of the emission spectrometer (12 nm/min), as described previously (11). At potentials where they could be obtained, steady-state EL spectra were essentially identical to those generated by the pulse technique.

Instantaneous EL efficiencies were determined as described previously (3). The total emitted energy per pulse measured with an EG&G Model 550-3 pulse integration module was converted to 600-nm photons using the manufacturer's correction factor at that wavelength.

Results and Discussion

Single-crystal samples of cubic n-ZnSe doped with Al (~ 2 ppm) and having carrier concentrations of $\sim 10^{17}$ - 10^{18} cm $^{-3}$ were employed in these studies. Sections below describe the PL properties of these solids, their perturbation by PEC parameters, and EL from the solids.

PL Spectra. Near-uv excitation of n-ZnSe:Al crystals produces effulgent, orange emission. The 295 K PL spectrum of the material, Fig. 1, is dominated by a broad band (FWHM ~ 115 nm) with $\lambda_{\text{max}} \sim 600$ nm; a weaker, sharper band (FWHM ~ 10 nm) peaking at ~ 460 nm is also present. The latter transition, whose intensity is reported to be very sensitive to preparative conditions (15), occurs near the band gap energy ($E_g \sim 2.7$ eV (16)). Although the band's origin in our samples is unknown, its designation as edge emission appears apt based on its energetic proximity to E_g and its temperature dependence: Fig. 1 indicates that the band blue shifts by ~ 0.09 eV to 445 nm upon cooling to 77 K, consistent with the temperature coefficient of -4.1×10^{-4} eV/K reported for exciton emission from cathodoluminescence studies (16b).

An intense orange band at ~ 630 nm has been reported for many ZnSe samples and assigned as self-activated (SA) PL; the transition is believed to involve a deep trapping level arising from a complex based on a Zn vacancy, V_{Zn} , and a next-neighbor donor impurity such as Al_{Zn} (Al on a Zn site) (17). Our spectra are somewhat more complex, but accord well with spectra reported by Bouley et al (15). Figure 1 reveals that the band at 600 nm seen at 295 K splits into two bands with $\lambda_{\text{max}} \sim 630$ and 550 nm at 77 K. The former, likely the SA band, has been assigned to complexes involving a neutral ($V_{\text{Zn}}\text{Al}_{\text{Zn}}$) or ionized defect ($V_{\text{Zn}}\text{Al}_{\text{Zn}}^-$), while the latter was ascribed to a defect involving Al and an alkali metal impurity (15). For convenience, we will refer to the 600-nm transition as a SA band, although we emphasize that its origin is not fully established in our samples.

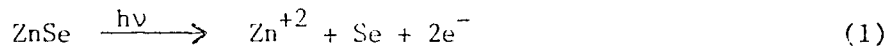
PL Efficiency. As previously noted, samples of n-ZnSe:Al are highly emissive. We have employed a technique to obtain ϕ_r values which, using a common geometry, compares light reflected from a nonabsorbing material with light reflected and emitted from a sample (12). Table I presents a compilation of measured ϕ_r values obtained in air for the SA emission using several different excitation wavelengths. The tabulated values, uncorrected for self-absorption and internal reflectivity, are substantial, ranging from ~2-5%. Large radiative efficiencies are also supported by the modest doubling of ϕ_r observed when samples are cooled to 77 K. Similar efficiencies and thermal behavior were reported for the ZnSe:Al samples studied by Bouley et al (15). The decline in ϕ_r with excitation wavelength, Table I, suggests the presence of a nonemissive near-surface region: Reported absorptivities increase substantially below 460 nm (18), so that a nonemissive layer is expected to reduce ϕ_r as it absorbs larger fractions of incident light.

PL Decay Times. Time-resolved PL properties were studied in air using the 337- and 460-nm outputs of a N_2 laser and N_2 -pumped dye laser, respectively. Measurements of the edge PL band were limited by the duration of the laser pulse, indicating a decay time of ~ 7 ns. A similar limitation was observed for the rise time of the SA band and its initial decay. After the peak intensity of the band had dropped ~30%, however, a much longer nonexponential decay was observed with typical $\tau_{1/e}$ values being ~ 1 μ s. These properties were independent of the excitation wavelengths employed and of the PL wavelength monitored.

Mechanistically, the different temporal behavior of the edge and SA bands is an important result in that it indicates that the corresponding excited states are not thermally equilibrated (19). Initiation of the SA emission is also addressed by the data. Although the rapid rise time for the SA band could reflect population via the excited state responsible for edge emission, our data are also consistent with population from a yet higher-energy state when ultraband gap wavelengths are employed; in the latter case, the strong lattice

coupling characteristic of deep traps provides a relaxation mechanism for rapid population of the SA state in parallel with population of the state leading to edge emission. Excited-state communication by either of the schemes outlined is also supported by steady-state measurements using the near uv lines of an Ar^+ laser; over an incident intensity range of $\sim 10^{-2}$ to 10^1 mW/cm^2 , the intensities of the edge and SA PL bands maintain a constant ratio.

PEC Properties. Although n-ZnSe has been used as an electrode in PEC's (18,20), the material has not, to our knowledge, been stabilized to the extent that it can be used for efficient conversion of optical energy to electricity; decomposition according to eq. (1) has previously been observed in several electrolytes (20a,b,f). The ability to stabilize n-CdX (X = S, Se, Te) electrodes with polychalcogenide



electrolytes suggested their use with n-ZnSe electrodes (9). In an initial experiment with sulfide electrolyte ($1\text{M OH}^-/1\text{M S}^{2-}$), decomposition still obtained: photocurrent fell rapidly, and pitting of the surface occurred. However, PEC's constructed from n-ZnSe:Al, a Pt counterelectrode and (di)selenide or (di)telluride electrolyte were stable. Table II demonstrates that little electrode weight loss accompanies long-term experiments in these electrolytes. Other evidence of stability includes relatively constant photocurrents and lack of surface damage in the prolonged experiments, as well as observation of competitive electrolyte oxidation (9).

We obtained photoaction spectra of our samples near short circuit in a transparent selenide electrolyte. Figure 2 reveals that, as expected, photocurrent rises sharply at $\sim 460 \text{ nm}$, roughly the band gap energy. The enhanced efficiency of e^--h^+ pair separation with decreasing wavelength is consistent with the reported trend in absorptivities (18) and with the decline in electric field strength with distance from the interface (21).

Current-voltage curves, shown in Figure 3, reveal that photocurrent in diselenide electrolyte onsets at ~ 2.0 V vs. SCE at moderate light intensities of ~ 10 mW/cm², yielding an open-circuit voltage of ~ 1.0 V. The photocurrent quantum efficiency, ϕ_x , is relatively low for these PEC's. Table I shows that even the least deeply penetrating wavelength, 366 nm, yields a short-circuit ϕ_x value of only ~ 0.50 . We attribute the low ϕ_x values to narrow depletion widths, W , and short hole diffusion lengths, L_p , in these materials: W is calculated to be $\sim 300-1000$ Å at short-circuit in our materials (22), and L_p has been reported to be only $\sim 10^2$ Å for comparably-doped ZnSe materials (20e). We estimate from PL data (vide infra) that the 366-nm absorptivity of ZnSe is $\sim 6-8 \times 10^4$ cm⁻¹ so that a significant fraction of $e^- - h^+$ pairs would be created beyond the depletion region where holes can be collected by diffusion into the drift region. Despite the modest ϕ_x values, Table I demonstrates that n-ZnSe:Al-based PEC's can still yield substantial efficiencies for the conversion of monochromatic light to electricity, values of $\sim 5-7\%$ for 366-nm excitation being typical. In the protracted experiments of Table II, energy conversion efficiencies of $\sim 3-4\%$ (366-nm experiments) were sustained for several days.

Of particular interest to us are changes in PL properties which accompany the use of the semiconductor as an electrode. Figure 4 demonstrates that in passing from open circuit to short circuit, the two PL bands are quenched roughly in parallel by the applied electric field. The spectral distribution is invariant over the potential range of Figure 3, permitting changes in PL intensity to be monitored at a single wavelength. Simultaneous measurements of current, PL intensity, and potential (iLV) data are illustrated in Figure 3 and summarized in Table I. The table reveals that PL quenching obtains with all of the excitation wavelengths employed.

Quenching of semiconductor PL by applied potential is a well-documented phenomenon in both semiconductor/metal- (6,23) and PEC-based (2,3) Schottky-barrier systems. A dead-layer model which quantifies PL quenching in the solid-state systems has recently been found applicable to PEC's based on n-CdSe and n-GaAs (4,5). In its simplest form, the model states that $e^- - h^+$ pairs formed within some fraction of the depletion width are swept apart by the field and do not contribute to PL. The mathematical form of the model is given by eq. (2) where D

$$\frac{\phi_r}{\phi_{r_{FB}}} = \exp(-\alpha'D) \quad (2)$$

is the dead-layer thickness; ϕ_r and $\phi_{r_{FB}}$ are the radiative quantum efficiencies at an in-circuit potential and at flat-band potential (approximated here as the open-circuit potential); and $\alpha' = \alpha + \beta$ with α and β the solid's absorptivities for the exciting and emitted light, respectively.

The dead-layer model was recently shown to be applicable to PL from a Au-ZnSe Schottky diode; PL intensity-voltage curves obtained with 442-nm light could roughly be fit by assuming that D has a functional dependence like that of W ($W \propto (V - V_{FB})^{\frac{1}{2}}$) (6). For the n-ZnSe:Al-based PEC's, PL quenching curves like that shown in Figure 3 can be similarly fit, although discrepancies occur near open circuit. Such discrepancies, also noted for n-GaAs-based PEC's, may indicate that potential applied in this regime is partitioned between the semiconductor and the Helmholtz layer (4).

Another quantitative test of the dead-layer model, independence of D on optical penetration depth, is presently precluded by a lack of reliable absorptivities for n-ZnSe:Al. However, qualitative accord is indicated by the enhanced PL quenching at short circuit with decreasing wavelength and penetration depth, Table I. If the dead-layer model is assumed applicable to these PEC's, it yields, using $\alpha \sim 3 \times 10^4 \text{ cm}^{-1}$ for 436-nm light (6), absorptivities of $\sim 4 \times 10^4$ and $6 \times 10^4 \text{ cm}^{-1}$ at 405 and 366 nm, respectively.

The effect of carrier concentration on PL quenching was also qualitatively consistent with the dead-layer model. As was found in the solid-state study (6), more resistive samples, prepared by heating ZnSe:Al in an evacuated ampule with Se, exhibited greater PL quenching, as shown in Table I. The wider electric fields of these samples were also manifest in larger ϕ_x values. Taken as a unit, we believe our data provide good evidence for describing PL quenching in n-ZnSe:Al-based PEC's in terms of a dead-layer model.

A final point of interest concerns the parallel quenching of the two PL bands illustrated in Figure 4. Although we are unable to definitively establish the mechanism for populating the SA state (vide supra), the parallel quenching is consistent with separation of $e^- - h^+$ pairs prior to population of this state.

EL Properties. We have found that n-ZnSe:Al electrodes mimic other II-VI electrodes (3) in exhibiting EL when used as a cathode in aqueous, alkaline, peroxydisulfate electrolyte (24). The key step involved in populating the emissive excited state has been proposed to be hole injection by SO_4^{2-} radical anions formed by reduction of $S_2O_8^{2-}$ (25). As in previous studies, we have obtained EL spectra using a pulse technique: while the emission monochromator is swept, the electrode is pulsed repetitively between a potential where no current is observed (0.0 V for 8 s) and a potential sufficiently cathodic to initiate EL (1-s pulse). We find that EL is initiated to the dark-adapted eye at ~ -1.7 V vs. SCE, roughly the onset of dark cathodic current in the electrolyte of 5M OH^- /0.1 M $S_2O_8^{2-}$.

Figure 5 presents the EL spectrum of an n-ZnSe:Al electrode. Both the edge and SA emission bands are evident, and a comparison with Fig. 1 indicates that the relative intensities of the bands are similar in the two spectra. The overall spectral similarity indicates that the same two emissive excited states are populated in both experiments.

Besides spectral distributions, we have also measured lower-limit integrated EL efficiencies, $\bar{\phi}_{EL}$, using techniques and approximations previously described (3). For n-ZnSe:Al electrodes, we obtain $\bar{\phi}_{EL}$ values of $\sim 10^{-6}$ and 10^{-4} at -1.8 and -2.2 V vs. SCE, respectively. These numbers are of interest because $\bar{\phi}_{EL}$ (photons emitted per holes injected) can be factored into an efficiency for excited-state population, ϕ_{ES} (excited states populated per holes injected) and the PL radiative efficiency, ϕ_r (photons emitted per excited states populated). Samples of n-CdS_xSe_{1-x} ($0 \leq x \leq 1$) exhibit $\bar{\phi}_{EL}$ and ϕ_r values which are nearly equal, suggesting ϕ_{ES} is near unity for these samples. In contrast, our $\bar{\phi}_{EL}$ values for n-ZnSe:Al are lower than the measured ϕ_r of $\sim 10^{-1}$ - 10^{-2} by a factor of 10^{-2} - 10^{-4} . The discrepancy in the two efficiencies may be due to a low value of ϕ_{ES} but more likely reflects the different spatial regions involved in the two modes of excited-state population. In particular, EL is expected to originate, on average, from nearer the semiconductor surface than PL, owing to its initiation by interfacial charge transfer. A lower ϕ_r value for the (near-)surface region due to nonradiative surface recombination could then account for the observed low EL efficiencies. Such a non-emissive near-surface region has already been suggested to account for the variation of PL efficiency with excitation wavelength. Reduction of the electrode surface during the EL experiment (3) may also contribute to the discrepancy.

Acknowledgment. This work was generously supported by the Office of Naval Research. A.B.E. gratefully acknowledges support as an Alfred P. Sloan Fellow (1981-83). Dr. Brian Fitzpatrick of North American Philips is thanked for generously providing the samples used in this study as well as for helpful discussions. Alan Huelsman and William Hobson are thanked for experimental assistance and helpful discussions.

References

1. (a) A. Heller, Acc. Chem. Res., 14, 154 (1981); (b) A. J. Bard, Science, 207, 139 (1980); (c) M. S. Wrighton, Acc. Chem. Res. 12, 303 (1979); (d) A. J. Nozik, Ann. Rev. Phys. Chem. 29, 189 (1978).
2. A. B. Ellis, J. Chem. Ed., 60, 332 (1983) and references therein.
3. H. H. Streckert, J. Tong, M. K. Carpenter, and A. B. Ellis, This Journal, 129, 772 (1982) and references therein.
4. W. S. Hobson and A. B. Ellis, J. Appl. Phys., 54, 5956 (1983).
5. M. Tomkiewicz, private communication.
6. K. Ando, A. Yamamoto, and M. Yamaguchi, Jpn. J. Appl. Phys. 20, 679 (1981).
7. O. Lindberg, Proc. of the I.R.E. 40, 1414 (1952).
8. B. R. Karas and A. B. Ellis, J. Am. Chem. Soc. 102, 968 (1980).
9. A. B. Ellis, S. W. Kaiser, J. M. Bolts, and M. S. Wrighton, J. Am. Chem. Soc., 99, 2839 (1977).
10. W. S. Hobson and A. B. Ellis, Appl. Phys. Lett. 41, 891 (1982).
11. H. H. Streckert, B. R. Karas, D. J. Morano, and A. B. Ellis, J. Phys. Chem., 84, 3232 (1980).
12. M. S. Wrighton, D. S. Ginley, and D. L. Morse, J. Phys. Chem. 78, 2229 (1974).
See ref. 3 for previous applications of the technique to semiconductor electrodes.
13. M. M. Olken, R. N. Biagioni, and A. B. Ellis, Inorg. Chem., 22, 000 (1983).
14. M. K. Carpenter, H. H. Streckert, and A. B. Ellis, J. Solid State Chem., 45, 51 (1982).
15. J. C. Bouley, P. Blanconnier, A. Herman, Ph. Ged, P. Henoc, and J. P. Noblanc, J. Appl. Phys. 46, 3549 (1975).

14

16. (a) M. Cardona, J. Appl. Phys. 32S, 2151 (1961); (b) B. Sermage, Solid-State Electron. 21, 1361 (1978).
17. (a) D. Curie and J. S. Prener in "Physics and Chemistry of II-VI Compounds," M. Aven and J. S. Prener, Editors, Chap. 9.4, North-Holland Publishing Co., Amsterdam (1967) and references therein. (b) S. Iida, J. Phys. Soc. Jpn. 25, 177 (1968); (c) G. Jones and J. Woods, J. Luminescence, 9, 389 (1974); (d) S. Satoh and K. Igaki, Jpn. J. Appl. Phys. 22, 68 (1983).
18. P. Lemasson, A. Etcheberry, and J. Gautron, Electrochim. Acta, 27, 607 (1982).
19. (a) B. DiBartolo, "Optical Interactions in Solids," Ch. 18.3, John Wiley and Sons, New York (1968); (b) P. J. Wagner in "Creation and Detection of the Excited State," Part A, Vol. I, A. A. Lamola, Editor, Chapt. 4, Marcel Dekker, New York (1971).
20. (a) R. Williams, This Journal, 114, 1173 (1967); (b) J. Gautron, P. Lemasson, F. Rabago, and R. Triboulet, This Journal, 126, 1868 (1979); (c) P. Lemasson, J. Gautron, J.-P. Dalbéra, Ber. Bunsenges. Phys. Chem. 84, 796 (1980); (d) P. Lemasson, J.-P. Dalbera, and J. Gautron, J. Appl. Phys. 52, 6296 (1981); (e) J. Gautron and P. Lemasson, J. Crystal Growth, 59, 332 (1982); (f) B. S. H. Royce, F. Sánchez-Sinencio, R. Goldstein, R. Muratore, R. Williams, and W. M. Yim, This Journal, 129, 2393 (1982).
21. H. Gerischer, J. Electroanal. Chem. Interfacial Electrochem., 58, 263 (1975) and references therein.
22. A static dielectric constant of 8.7 was used in calculating W, ref. 20d.
23. R. E. Hollingsworth and J. R. Sites, J. Appl. Phys., 53, 5357 (1982) and references therein.
24. EL from n-ZnSe under anodic polarization has also been reported: J. Gautron, J.-P. Dalbera, and P. Lemasson, Surf. Sci. 99, 300 (1980).
25. (a) K. H. Beckmann and R. Memming, This Journal, 116, 368 (1969); (b) R. Memming, This Journal, 116, 785 (1969); (c) B. Pettinger, H. R. Schöppel, and H. Gerischer, Ber. Bunsenges. Phys. Chem. 80, 849 (1976).

Table I. PL properties and measurements of efficiency in n-ZnSe:Al-based PEC's^a

Electrode ^b	$\lambda_{ex, nm}^c$	Φ_r^d	Φ_x^e	$(1 - \frac{\Phi_r}{\Phi_{r,FB}})^f$	$\Phi_x @ \eta_{max}^g$	$E_v @ \eta_{max}, V^h$	η_{max}^i (%)
as received	366	0.02	0.50	0.16	0.35	0.85	7.2
	405	0.03	0.25	0.11	0.18	0.85	4.9
	436	0.04	0.18	0.09	0.14	0.90	4.2
	460	0.05					
treated	366		0.60	0.38	0.42	0.85	10.4
	405		0.31	0.17	0.23	0.77	5.3
	436		0.22	0.13	0.13	0.73	3.6

^aPL properties related to use of n-ZnSe:Al electrodes in PEC's. Most of the properties are derived from iLV curves generated with a three-electrode potentiostatic setup (n-ZnSe:Al working electrode, Pt foil counterelectrode and SCE reference electrode). To optimize transparency, experiments with 366-nm light were conducted in 10M KOH/0.25M Se_2^{2-} /0.001M Se_2^{2-} electrolyte; for 405- and 436-nm light, an electrolyte of 8M KOH/0.2M Te_2^{2-} /0.002M Te_2^{2-} was employed. The electrode, having an exposed surface area of $\sim 0.25\text{ cm}^2$, was excited with $\sim 0.5\text{-}2\text{ mW}$ of power.

^bThe n-ZnSe:Al sample was used either "as received" or treated with Se as described in the Experimental Section and text. ^cExcitation wavelength. A 150-W high-pressure Xe lamp or 200-W high-pressure Hg lamp equipped with interference filters was employed for Φ_r data and iLV curves, respectively.

^dRadiative quantum efficiencies obtained in air for the SA band. Values are uncorrected for self-absorption and internal reflectivity.

^eMeasured photocurrent quantum efficiency at -1.0 V vs. SCE. Values are uncorrected for solution absorption and reflective losses.

^fFractional PL quenching between -1.0 V vs. SCE and the flat-band potential, approximated here as the open-circuit potential. PL intensity was monitored at 600 nm.

^gMeasured photocurrent quantum efficiency at the potential corresponding to maximum optical-to-electrical energy conversion efficiency.

^hOutput voltage at the maximum energy conversion point. The diselenide and ditelluride redox potentials were -0.95 and -1.10 V vs. SCE, respectively.

ⁱ(Maximum electrical power out divided by input optical power) $\times 100$.

Table II. Stabilization of n-ZnSe:Al photoelectrodes^a

Exp't.	Electrolyte ^b	Electrode before	(mol x 10 ⁴) ^c	Electrons ^d (mol x 10 ⁴)	Avg i, ^e mA	t, h	Output Voltage, V	$\lambda_{ex, nm}$ ^f
1	Se _n ²⁻	0.81	0.80	2.06	0.063	87.5	0.36	366
2	Se _n ²⁻	1.80	1.68	3.72	0.075	133	0.75	366
3	Te _n ²⁻	0.88	0.84	3.19	0.100	85.5	0.63	436
4	Te _n ²⁻	1.25	1.23	2.46	0.055	120	0.55	436

^aAll experiments were run under N₂ in stirred solutions in a two-electrode PEC (working electrode and Pt foil counterelectrode) in diselenide or ditelluride electrolyte.

^bElectrolyte compositions are given in Table I. The initially colorless solutions became dark brown and deep purple as Se₂²⁻ and Te₂²⁻ were formed, respectively, during the course of the experiments. Final Se₂²⁻ and Te₂²⁻ concentrations were ~0.002 and 0.004 M, respectively.

^cMoles of crystal determined by weight before and after photoelectrochemistry. Crystals used in experiments 1, 2, and 3 chipped while being demounted and were not fully recovered. Surface areas were 0.08, 0.18, 0.09, and 0.12 cm² for the solids of expt's 1-4, respectively.

^dMoles of electrons in the external circuit determined by integrating photocurrent-time plots.

^eAverage photocurrent passed during experiment; for current densities, divide by the electrode areas given in footnote c.

^fExcitation wavelength provided by a 200-W high-pressure Hg lamp equipped with interference filters.

11

Figure Captions

Figure 1. Corrected, front-surface PL spectra of n-ZnSe:Al at 295 K (dashed line) and 77 K (solid line). Both spectra were taken at the same sensitivity (a 100-fold increase in sensitivity was used in scanning the 410-480-nm region). The sample was excited with identical intensities of 405-nm light without disturbing the experimental geometry.

Figure 2. Photoaction spectrum for a n-ZnSe:Al-based PEC in optically transparent selenide electrolyte; the electrode was held at -1.0 V vs. SCE. The plotted values of relative photocurrent have been corrected for variation in light intensity as a function of wavelength. Although the optical pathlength was minimized, the spectrum is not corrected for electrolyte absorption.

Figure 3. Photocurrent (bottom frame) and PL intensity (top frame) monitored at $\lambda_{\text{max}} \sim 600$ nm vs. potential for a n-ZnSe:Al electrode excited at 366 nm in 10 M KOH/0.25 M Se^{2-} /0.001M Se_2^{2-} electrolyte. The incident light irradiated the $\sim 0.2\text{-cm}^2$ exposed area of the electrode with ~ 0.60 mW of power. The iLV curves were generated using a pulse technique described in the Experimental Section. The electrolyte redox potential was -0.95 V vs. SCE.

Figure 4. Corrected PL spectra of a n-ZnSe:Al electrode excited with the near-uv lines (351, 364 nm) of an Ar^+ laser in the diselenide electrolyte of Figure 3. Curves A and B were taken at -2.0 V (open circuit) and -1.0 V vs. SCE, respectively. Both spectra were taken in an identical sample geometry.

Figure 5. Corrected EL spectra of an n-ZnSe:Al electrode obtained in 5M OH^- /0.1M $\text{S}_2\text{O}_8^{2-}$ electrolyte. The electrode was continuously pulsed between 0.00 V (8 s) and -2.0 V vs. SCE (1 s) while the emission spectrometer was swept at 12 nm/min. A 100-fold increase in sensitivity was used in scanning the 400-480-nm spectral region.

Figure 1 18

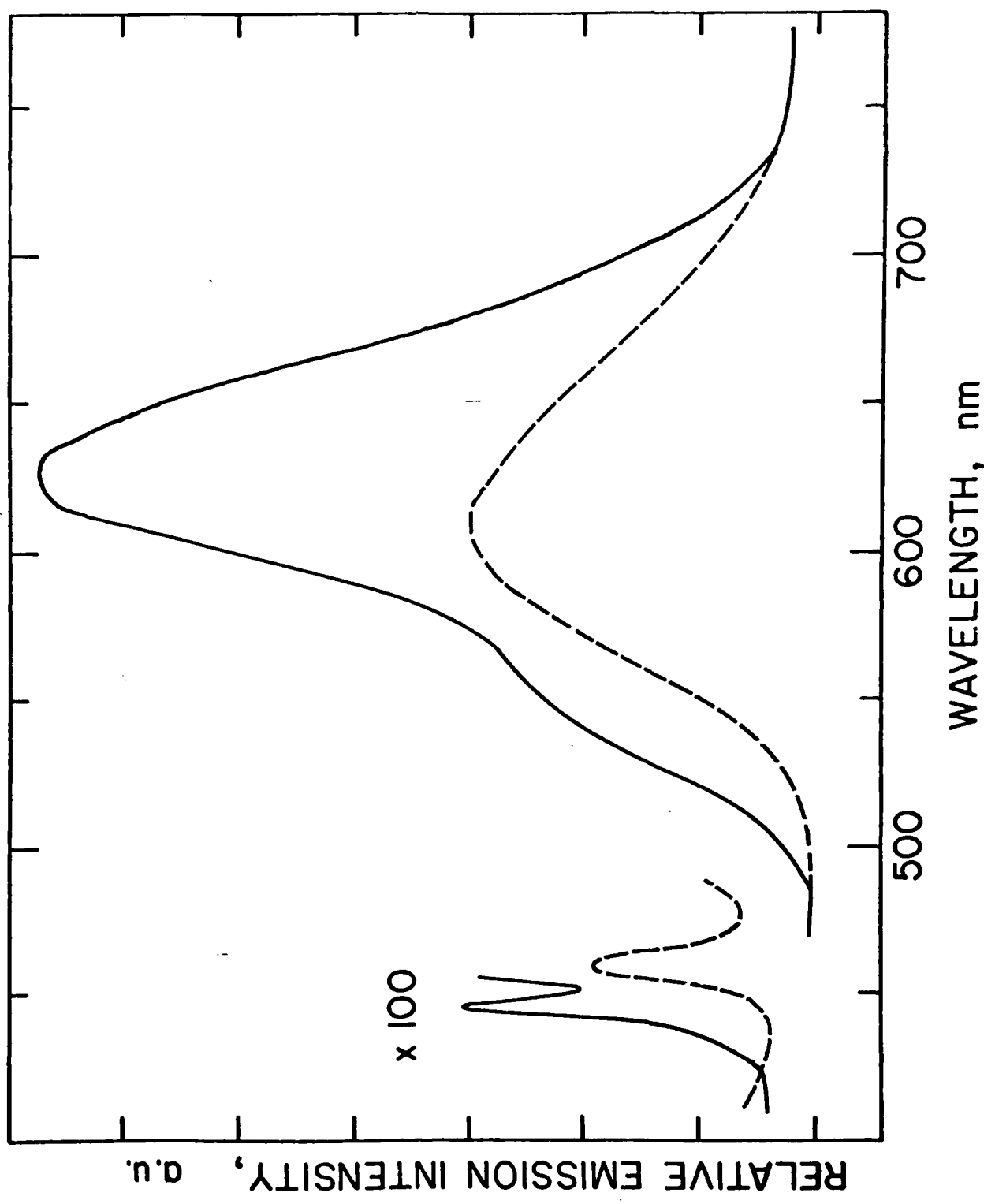


Figure 2 19

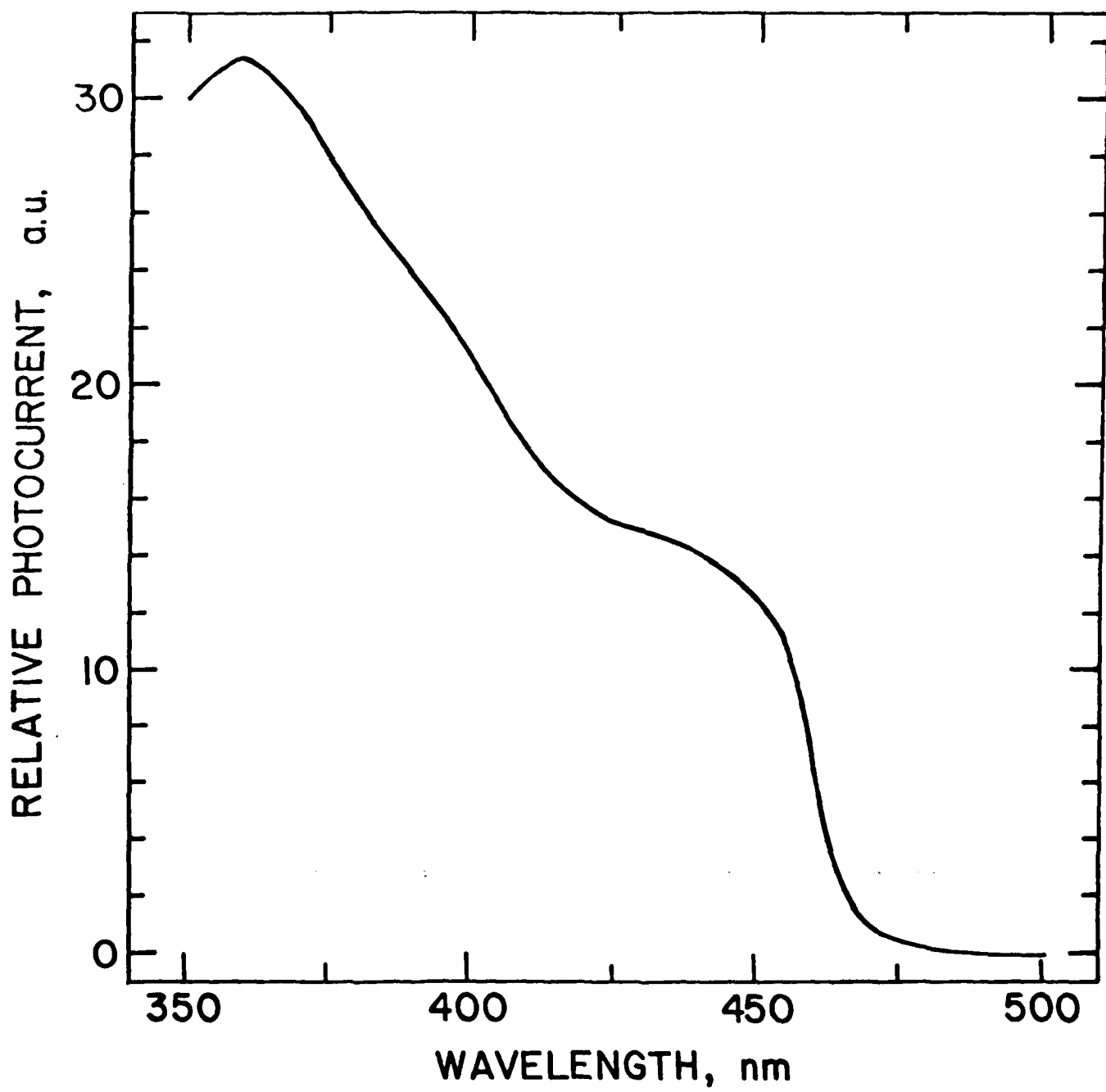


Figure 3

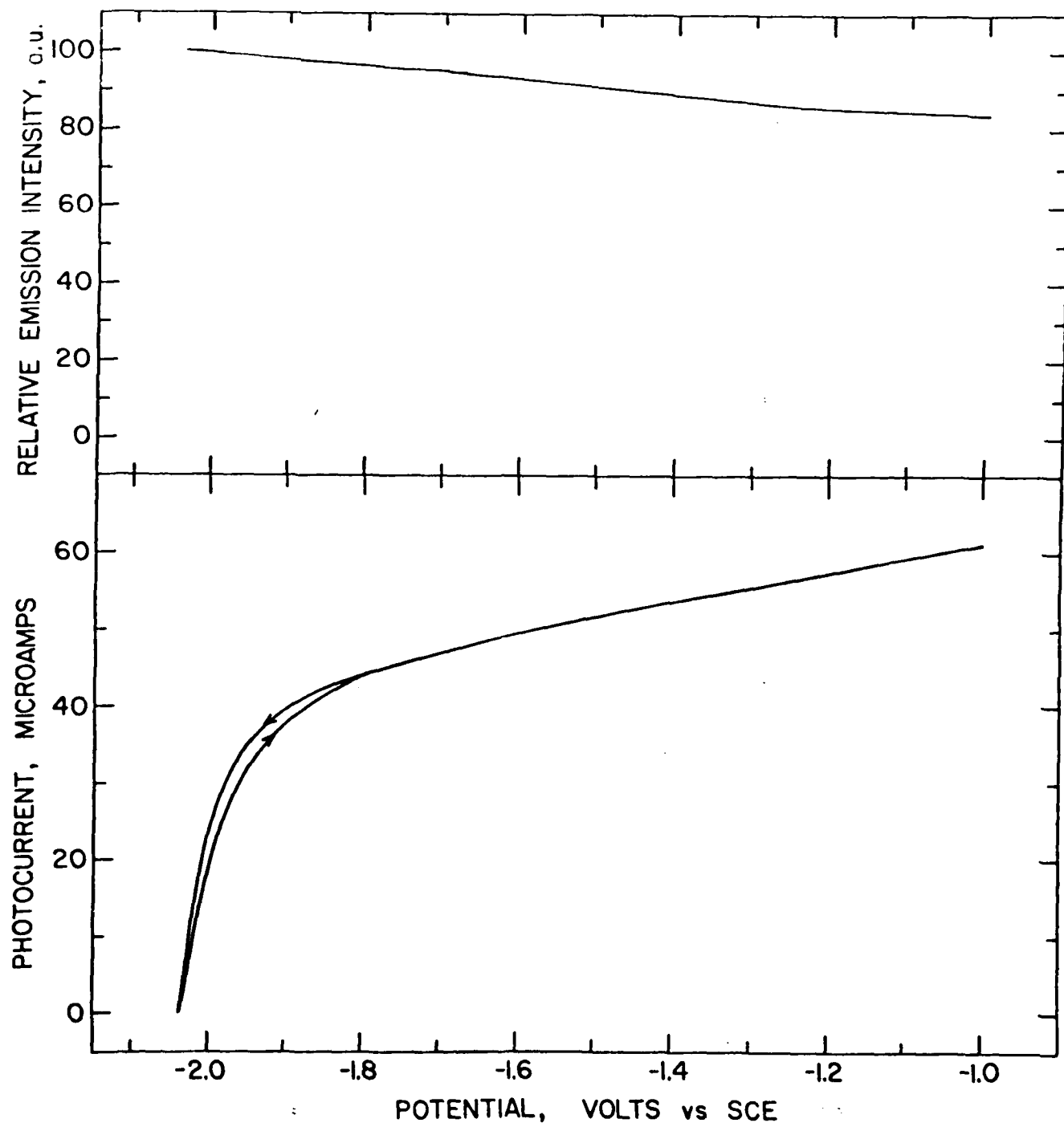


Figure 4

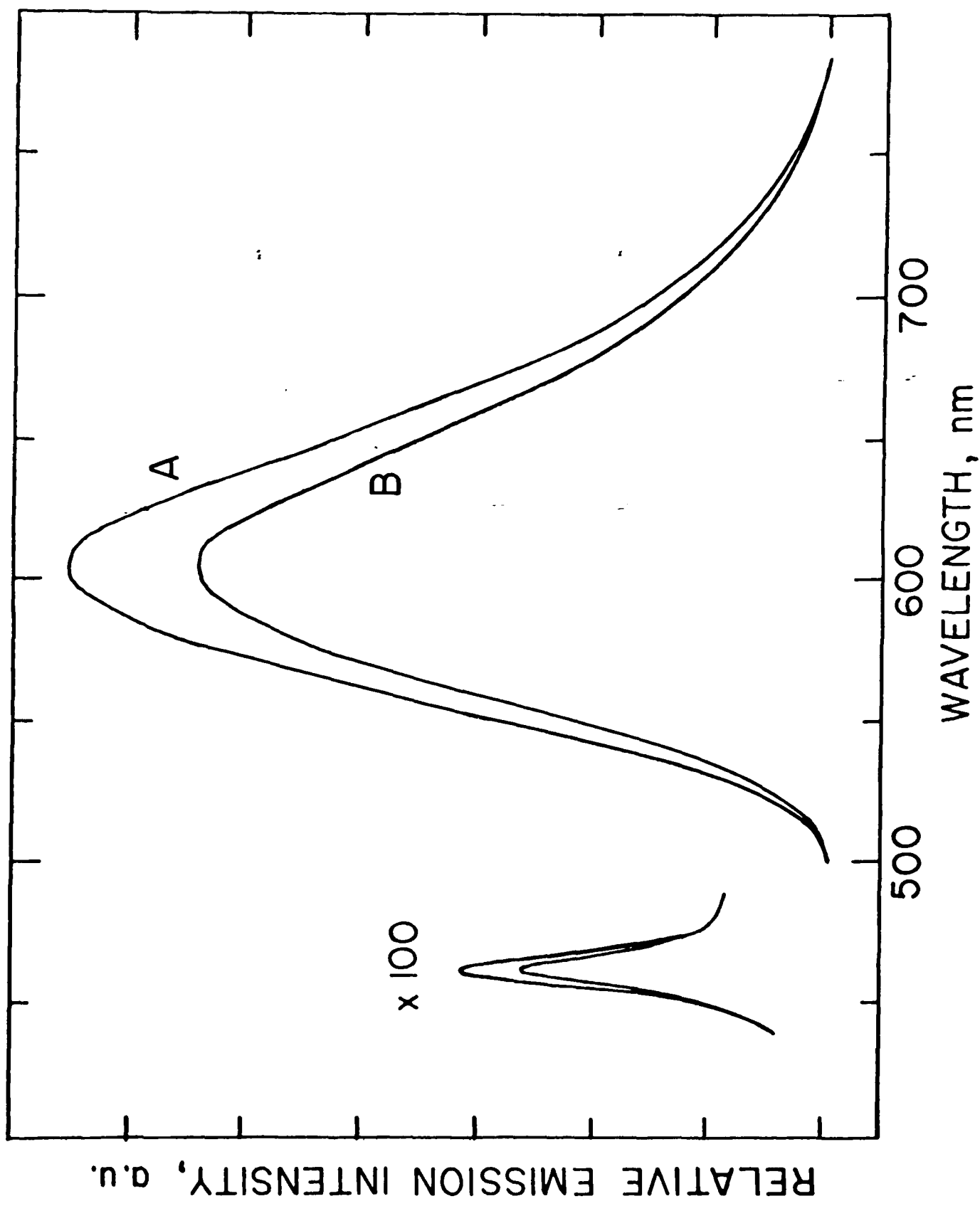
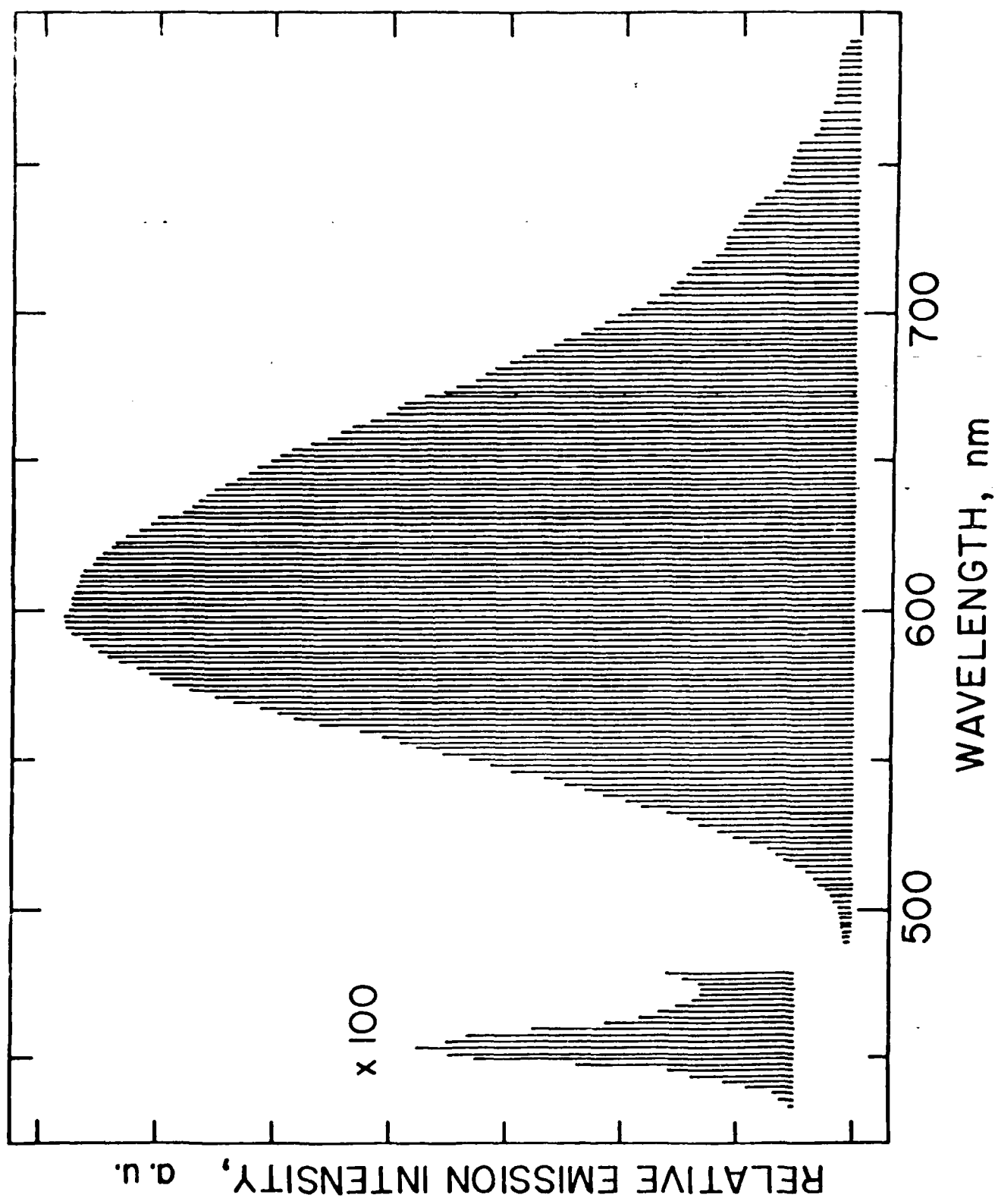


Figure 5



TECHNICAL REPORT DISTRIBUTION LIST, GEN

<u>No.</u>	<u>Copies</u>	<u>No.</u>	<u>Copies</u>
Office of Naval Research Attn: Code 413 300 North Quincy Street Arlington, Virginia 22217	2	Naval Ocean Systems Center Attn: Mr. Joe McCartney San Diego, California 92152	
ONR Pasadena Detachment Attn: Dr. R. J. Marcus 1030 East Green Street Pasadena, California 91106	1	Naval Weapons Center Attn: Dr. A. B. Amster, Chemistry Division China Lake, California 93555	
Commander, Naval Air Systems Command Attn: Code 310C (H. Rosenwasser) Department of the Navy Washington, D.C. 20360	1	Naval Civil Engineering Laboratory Attn: Dr. R. W. Drisko Port Hueneme, California 93401	
Defense Technical Information Center Building 5, Cameron Station Alexandria, Virginia 22314	12	Dean William Tolles Naval Postgraduate School Monterey, California 93940	
Dr. Fred Saalfeld Chemistry Division, Code 6100 Naval Research Laboratory Washington, D.C. 20375		Scientific Advisor Commandant of the Marine Corps (Code RD-1) Washington, D.C. 20380	
U.S. Army Research Office Attn: CRD-AA-IP P. O. Box 12211 Research Triangle Park, N.C. 27709	1	Naval Ship Research and Development Center Attn: Dr. G. Bosmajian, Applied Chemistry Division Annapolis, Maryland 21401	
Mr. Vincent Schaper DTNSRDC Code 2803 Annapolis, Maryland 21402	1	Mr. John Boyle Materials Branch Naval Ship Engineering Center Philadelphia, Pennsylvania 19112	
Naval Ocean Systems Center Attn: Dr. S. Yamamoto Marine Sciences Division San Diego, California 91232	1	Mr. A. M. Anzalone Administrative Librarian PLASTEC/ARRADCOM Bldg 3401 Dover, New Jersey 07801	

TECHNICAL REPORT DISTRIBUTION LIST, 359

<u>No.</u>	<u>Copies</u>	<u>Co1</u>
Dr. Paul Delashaw Department of Chemistry New York University New York, New York 10003	1	Dr. P. J. Hendra Department of Chemistry University of Southampton Southampton SOO 5NH United Kingdom
Dr. E. Yeager Department of Chemistry Case Western Reserve University Cleveland, Ohio 44106	1	Dr. Sam Perone Chemistry & Materials Science Department Lawrence Livermore National Lab. Livermore, California 94550
Dr. D. N. Bennion Department of Chemical Engineering Brigham Young University Provo, Utah 84602	1	Dr. Royce W. Murray Department of Chemistry University of North Carolina Chapel Hill, North Carolina 27514
Dr. R. A. Marcus Department of Chemistry California Institute of Technology Pasadena, California 91125	1	Naval Ocean Systems Center Attn: Technical Library San Diego, California 92152
Dr. J. J. Auborn Bell Laboratories Murray Hill, New Jersey 07974	1	Dr. C. E. Mueller The Electrochemistry Branch Materials Division, Research and Technology Department Naval Surface Weapons Center White Oak Laboratory Silver Spring, Maryland 20910
Dr. Adam Seller Bell Laboratories Murray Hill, New Jersey 07974	1	Dr. G. Goodman Johnson Controls 5757 North Green Bay Avenue Milwaukee, Wisconsin 53201
Dr. T. Katan Lockheed Missiles and Space Co., Inc. P. O. Box 504 Sunnyvale, California 94088	1	Dr. J. Boeckler Electrochimica Corporation Attn: Technical Library 2485 Charleston Road Mountain View, California 94040
Dr. Joseph Singer, Code 302-1 NASA-Lewis 21000 Brookpark Road Cleveland, Ohio 44135	1	Dr. P. P. Schmidt Department of Chemistry Oakland University Rochester, Michigan 48063
Dr. B. Brummer EIC Incorporated 55 Chapel Street Newton, Massachusetts 02158	1	
Library P. R. Mallory and Company, Inc. Northwest Industrial Park Burlington, Massachusetts 01803	1	

TECHNICAL REPORT DISTRIBUTION LIST, 359

<u>No.</u>	<u>Copies</u>	<u>No.</u> <u>Copies</u>	
Dr. H. Richsel Chemistry Department Rensselaer Polytechnic Institute Troy, New York 12181	1	Dr. R. P. Van Duyne Department of Chemistry Northwestern University Evanston, Illinois 60201	1
Dr. A. B. Ellis Chemistry Department University of Wisconsin Madison, Wisconsin 53706	1	Dr. B. Stanley Pons Department of Chemistry University of Alberta Edmonton, Alberta CANADA T6G 2G2	1
Dr. M. Wrighton Chemistry Department Massachusetts Institute of Technology Cambridge, Massachusetts 02139		Dr. Michael J. Weaver Department of Chemistry Michigan State University East Lansing, Michigan 48824	1
Larry E. Plew Naval Weapons Support Center Code 30736, Building 2906 Crane, Indiana 47522	1	Dr. R. David Rauh EIC Corporation 55 Chapel Street Newton, Massachusetts 02158	1
S. Ruby DOE (STOR) 600 E Street Providence, Rhode Island 02192	1	Dr. J. David Margerum Research Laboratories Division Hughes Aircraft Company 3011 Malibu Canyon Road Malibu, California 90265	1
Dr. Aaron Wold Brown University Department of Chemistry Providence, Rhode Island 02192	1	Dr. Martin Fleischmann Department of Chemistry University of Southampton Southampton SO9 5NH England	1
Dr. R. C. Chudacek McGraw-Edison Company Edison Battery Division Post Office Box 28 Bloomfield, New Jersey 07003	1	Dr. Janet Osteryoung Department of Chemistry State University of New York at Buffalo Buffalo, New York 14214	1
Dr. A. J. Bard University of Texas Department of Chemistry Austin, Texas 78712	1	Dr. R. A. Osteryoung Department of Chemistry State University of New York at Buffalo Buffalo, New York 14214	1
Dr. M. M. Nicholson Electronics Research Center Rockwell International 3370 Miraloma Avenue Anaheim, California	1		

TECHNICAL REPORT DISTRIBUTION LIST, 359

<u>No.</u>	<u>Copies</u>	<u>No</u>	<u>Copi</u>
Dr. Donald W. Ernst Naval Surface Weapons Center Code R-33 White Oak Laboratory Silver Spring, Maryland 20910	1	Mr. James R. Moden Naval Underwater Systems Center Code 3632 Newport, Rhode Island 02840	1
Dr. R. Nowak Naval Research Laboratory Code 6130 Washington, D.C. 20375	1	Dr. Bernard Spielvogel U. S. Army Research Office P. O. Box 12211 Research Triangle Park, NC 27709	1
Dr. John F. Houlihan Shenango Valley Campus Pennsylvania State University Sharon, Pennsylvania 16146	1	Dr. Denton Elliott Air Force Office of Scientific Research Bolling AFB Washington, D.C. 20332	1
Dr. D. F. Shriver Department of Chemistry Northwestern University Evanston, Illinois 60201	1	Dr. David Aikens Chemistry Department Rensselaer Polytechnic Institute Troy, New York 12181	1
Dr. D. H. Whitmore Department of Materials Science Northwestern University Evanston, Illinois 60201	1	Dr. A. P. B. Lever Chemistry Department York University Downsview, Ontario M3J1P3 Canada	1
Dr. Alan Bewick Department of Chemistry The University Southampton, SO9 5NH England		Dr. Stanislaw Szpak Naval Ocean Systems Center Code 6343 San Diego, California 95152	1
Dr. A. Homy NAVSEA-5433. NC #4 2541 Jefferson Davis Highway Arlington, Virginia 20362		Dr. Gregory Farrington Department of Materials Science and Engineering University of Pennsylvania Philadelphia, Pennsylvania 19104	
Dr. John Kincaid Kaman Sciences Corporation 1911 Jefferson Davis Hwy., Suite 1200 Arlington, Virginia 22202		Dr. Bruce Dunn Department of Engineering & Applied Science University of California Los Angeles, California 90024	

27

TECHNICAL REPORT DISTRIBUTION LIST, 359

N
Cop

<u>No.</u>	<u>Copies</u>
------------	---------------

M. L. Robertson
Manager, Electrochemical
and Power Sonics Division
Naval Weapons Support Center
Crane, Indiana 47522

1

Dr. T. Marks
Department of Chemistry
Northwestern University
Evanston, Illinois 60201

Dr. Elton Cairns
Energy & Environment Division
Lawrence Berkeley Laboratory
University of California
Berkeley, California 94720

1

Dr. D. Cipris
Allied Corporation
P. O. Box 3000R
Morristown, New Jersey 07960

Dr. Micha Tomkiewicz
Department of Physics
Brooklyn College
Brooklyn, New York 11210

1

Dr. M. Philpot
IBM Corporation
5600 Cottle Road
San Jose, California 95193

Dr. Lesser Blum
Department of Physics
University of Puerto Rico
Rio Piedras, Puerto Rico 00931

1

Dr. Donald Sandstrom
Washington State University
Department of Physics
Pullman, Washington 99164

Dr. Joseph Gordon, II
IBM Corporation
K33/281
5600 Cottle Road
San Jose, California 95193

1

Dr. Carl Kannewurf
Northwestern University
Department of Electrical Engineering
and Computer Science
Evanston, Illinois 60201

Dr. Robert Somoano
Jet Propulsion Laboratory
California Institute of Technology
Pasadena, California 91103

1

Dr. Edward Fletcher
University of Minnesota
Department of Mechanical Engineering
Minneapolis, Minnesota 55455

Dr. Johann A. Joebstl
USA Mobility Equipment R&D Command
DRDME-EC
Fort Belvoir, Virginia 22060

1

Dr. John Fontanella
U.S. Naval Academy
Department of Physics
Annapolis, Maryland 21402

Dr. Judith H. Ambrus
NASA Headquarters
M.S. RTS-6
Washington, D.C. 20546

1

Dr. Martha Greenblatt
Rutgers University
Department of Chemistry
New Brunswick, New Jersey 08903

Dr. Albert R. Landgrebe
U.S. Department of Energy
M.S. 6B025 Forrestal Building
Washington, D.C. 20595

1

Dr. John Wassib
Kings Mountain Specialties
P. O. Box 1173
Kings Mountain, North Carolina 28086

TECHNICAL REPORT DISTRIBUTION LIST, 359

<u>No.</u>	<u>Copies</u>	<u>Co</u>
Dr. J. J. Brophy University of Utah Department of Physics Salt Lake City, Utah 84112	1	
Dr. Walter Roth Department of Physics State University of New York Albany, New York 12222	1	
Dr. Thomas Davis National Bureau of Standards Polymer Science and Standards Division Washington, D.C. 20234	1	
Dr. Charles Martin Department of Chemistry Texas A&M University	1	
Dr. Anthony Sammells Institute of Gas Technology 3424 South State Street Chicago, Illinois 60616	1	
Dr. H. Tachikawa Department of Chemistry Jackson State University Jackson, Mississippi 39217	1	
Dr. W. M. Risen Department of Chemistry Brown University Providence, Rhode Island	1	